First-principles study of the equilibrium structures of Si_n clusters

1998 J. Phys.: Condens. Matter 10 5851

(http://iopscience.iop.org/0953-8984/10/26/013)

J. Phys.: Condens. Matter **10** (1998) 5851–5860. Printed in the UK PII: S0953-8984(98)90313-7

First-principles study of the equilibrium structures of Si_n clusters

Ji-Wook Jeong, In-Ho Lee, J H Oh and K J Chang

Department of Physics, Korea Advanced Institute of Science and Technology, 373-1, Kusung-dong, Yusung-ku, Taejon, Korea

Received 5 January 1998, in final form 24 March 1998

Abstract. We investigate the atomic structure of Si_n ($n = 9$–14) clusters using the first-principles pseudopotential method within the local-density-functional approximation (LDA). The equilibrium geometries of small clusters with $n \leqslant 12$ tend to be capped prismatic structures. For $n = 13$, we find a surface-like metallic compact structure which is derived from a capped icosahedron and competes with a stable trigonal prism, while this structure is the most stable for $n = 14$. These results are compatible with the observed stability of Si_{13} and Si_{14}, as compared to Si_n clusters with nearby values of n, against chemical reactions with simple molecules. The effect of electron–electron correlations on the energetics of isomers with $n = 13$ is examined through variational quantum Monte Carlo calculations, and the LDA energy ordering remains unchanged, consistently with previous diffusion quantum Monte Carlo calculations.

In the last few decades, covalently bonded semiconductor clusters have attracted much attention because of the significant dependence of their stability and reactivity on their specific size. For simple-metal clusters, the stability of which is mainly determined by the kinetic energy of electrons in a jellium droplet, the structural trend has been successfully described using the jellium approximation [1] as well as by means of first-principles calculations [2]. On the other hand, the stability of semiconductor clusters strongly depends on the atomic positions because of the covalent nature of the bonding, so a more realistic model beyond the jellium approximation is required [3]. Of special interest are the properties of Si_n clusters; only for small values of n have the equilibrium structures been identified theoretically and experimentally [4–7]. Since the computational demand grows quickly as the size of the cluster increases, our understanding of the ground states is still far from complete for large clusters. Among Si_n clusters, those with $n = 13$ and 14 have recently been focused on, because their chemical reactivities with several reactants are considerably lower than those for clusters with nearby values of n [8, 9], while in the reaction with C_2H_4, the inertness of Si_{13}^+ is more significant than that of Si_{14}^+. Despite several theoretical investigations based on empirical potentials, classical force fields, and purely quantum mechanical methods, no consensus has been reached on the equilibrium structure of Si_{13} [10–17]. Since the atom-centred icosahedron has the highest coordination number among all possible configurations, this structure was thought likely to be the ground-state geometry, and this was verified by empirical potential calculations [10]. In contrast, the local-density-functional approximation (LDA) approach predicted a trigonal antiprism as the lowest-energy state [18]. A more accurate treatment of electron–electron correlations using quantum Monte Carlo methods confirmed the validity of the LDA energy ordering

0953-8984/98/265851+10$19.50

for different structures [19], although it was suggested that the correlation could make the icosahedral structure more stable than the trigonal one [20]. Thus, to our knowledge, there has been no satisfactory explanation of why the chemical reactivity of Si_n^+ clusters depends strongly on their sizes.

In this paper, we present the results of first-principles calculations for the energetics of various isomers in Si_n ($n = 9$–14) clusters and discuss the structural characteristics of each cluster. We find that for $n \leqslant 12$, trigonal prismatic structures are more stable than octahedral and icosahedral ones. For $n = 13$, the surface-like compact geometry derived from a capped icosahedron is comparable in energy to the prismatic structure, while a similar surface-like structure is the most stable one for $n = 14$. This structural compactness and the resulting metallic bonding may cause the lower chemical reactivities for Si_{13}^+ and Si_{14}^+.

To determine the stable geometry of each isomer considered, we perform total-energy calculations based on an accurate and efficient first-principles pseudopotential method [21] within the local-density-functional approximation [22]. We employ the Ceperley and Alder form for the exchange–correlation potential as parametrized by Perdew and Zunger [23]. Norm-conserving nonlocal pseudopotentials are generated using the scheme of Troullier and Martins and the separable form of Kleinman and Bylander is constructed [24]. The total energy is calculated in momentum space using a simple cubic supercell with a volume of 8000 au. The wave functions are expanded in a plane-wave basis set with a kinetic energy cut-off of 10 Ryd. Increasing the kinetic energy cut-off up to 30 Ryd and the unit-cell size, we find the maximum error in estimating relative binding energies to be less than 0.02 eV per atom. Since the number of isomers dramatically increases as the cluster size increases, the determination of the globally minimized structure is very difficult for large clusters. For Si_9–Si_{14} clusters, we examine numerous isomers and fully relax the ionic positions by calculating the Hellmann–Feynman forces until the forces are less than 3 mRyd/a_B, where a_B is the Bohr radius. On the basis of the bonding nature of cluster isomers and their electronegativities, we discuss the energetics and chemical reactivity.

We also investigate the effect of electron correlation on the structural properties of the Si_{13} cluster using the variational quantum Monte Carlo (VQMC) method [25], which enables us to evaluate the correlation energy accurately. In a system with N valence electrons, the expectation value of the Hamiltonian H for the many-body wave function $\Psi(\boldsymbol{r}_1, \ldots, \boldsymbol{r}_N)$ is given by a $3N$-dimensional integral, and evaluated by taking the random-walk average in the configuration space:

$$\int \Psi^*(\boldsymbol{r}_1, \ldots, \boldsymbol{r}_N)\hat{H}\Psi(\boldsymbol{r}_1, \ldots, \boldsymbol{r}_N)\ \mathrm{d}\boldsymbol{r}_1\ \cdots\ \mathrm{d}\boldsymbol{r}_N \simeq \frac{1}{N_w}\sum_{i=1}^{N_w}\left\{\frac{\hat{H}\Psi}{\Psi}\right\}_{\boldsymbol{R}=\boldsymbol{R}_i}|\Psi(\boldsymbol{R}_i)|^2 \qquad (1)$$

where N_w is the number of steps in the random walk, and the $\boldsymbol{R}_i$ are the points in the configuration visited by the walk. The trial function used here is of the Slater–Jastrow form

$$\Psi(\boldsymbol{R}) = \Psi_J D^{\uparrow}(\boldsymbol{R})D^{\downarrow}(\boldsymbol{R}) \qquad (2)$$

where $D^s(\boldsymbol{R})$ is the Slater determinant of single-electron orbitals with spin s. The Jastrow factor Ψ_J is expressed as follows:

$$\Psi_J(\boldsymbol{R}) = \exp\left[\sum_{(s,i)=(\uparrow,1)}^{(\downarrow,N)}\xi_s(\boldsymbol{r}_i^s) - \sum_{(\uparrow,1)\leqslant(s,i)<(s',j)}^{(\downarrow,N)}u_{ss'}(r_{ij})\right] \qquad (3)$$

where the two-body term $u(r_{ij})$ depends only on the distance r_{ij} between the electrons. The one-body Jastrow term $\xi(\boldsymbol{r})$ is used for a variational adjustment of the electron charge density in the presence of the two-body term $u(r_{ij})$, and in our calculations the standard

Table 1. The average bond length a_0 (in au), the average coordination number $\bar{N}_c$, the energy gap ΔE (in eV) between the HOMO and LUMO states, and the LDA binding energies E_b^{LDA} (in eV/atom) for Si_n, $9 \leqslant n \leqslant 12$. The VQMC binding energies of Si_{13} are compared with the diffusion quantum Monte Carlo calculations of reference [19]. The GGA calculational results are included in parentheses.

	Structure	a_0	$\bar{N}_c$	ΔE	E_b^{LDA}	E_b^{VQMC}
Si_9	Tricapped trigonal prism I	4.75	4.67	0.43	3.96	
	Tricapped trigonal prism II	4.63	4.22	0.22	4.07	
	Tricapped trigonal prism III	4.69	4.67	0.01	4.08	
	Tricapped octahedron	4.66	4.44	0.92	4.13	
	Bicapped pentagonal bipyramid I	4.76	5.11	1.50	4.18	
	Bicapped pentagonal bipyramid II	4.68	4.67	2.02	4.25	
Si_{10}	Bicapped tetragonal antiprism	4.73	4.80	1.13	4.23	
	Tetracapped octahedron	4.64	4.80	2.12	4.32	
	Tetracapped trigonal prism	4.67	4.80	2.07	4.37	
Si_{11}	Capped pentagonal antiprism	4.67	4.55	0.43	4.11	
	Tricapped tetragonal antiprism	4.66	4.73	1.09	4.29	
	Pentacapped trigonal prism I	4.69	4.91	0.01	4.29	
	Pentacapped trigonal prism II	4.64	4.91	1.80	4.32	
Si_{12}	Distorted icosahedron	4.78	5.00	0.90	4.14	
	Tetracapped tetragonal prism	4.70	4.67	0.52	4.17	
	Hexacapped trigonal antiprism	4.60	4.00	0.92	4.27	
	Hexacapped trigonal prism	4.65	4.50	2.17	4.34	
Si_{13}	Capped icosahedron	4.76	5.08	0.90	4.18	
	Distorted core-based icosahedron	4.82	5.54	1.29	4.15	2.95
		(4.90)	(5.54)	(1.33)	(3.61)	
					3.98[a]	3.12[a]
	Surface-like distorted icosahedron	4.74	5.08	1.07	4.34	3.25
		(4.81)	(5.08)	(1.09)	(3.79)	
	Heptacapped trigonal antiprism	4.65	4.62	1.62	4.33	3.22
		(4.71)	(4.62)	(1.59)	(3.78)	
					4.28[a]	3.41[a]
	Heptacapped trigonal prism I	4.67	4.77	1.37	4.32	
	Heptacapped trigonal prism II	4.66	4.62	1.54	4.34	
	Heptacapped trigonal prism III	4.66	4.77	1.47	4.38	3.38
		(4.74)	(4.77)	(1.42)	(3.83)	
Si_{14}	Distorted bicapped hexagonal prism	4.73	5.00	1.22	4.30	
	Octacapped trigonal antiprism	4.72	5.14	0.28	4.31	
	Octacapped trigonal prism I	4.84	5.57	0.38	4.22	
	Octacapped trigonal prism II	4.70	5.14	0.65	4.31	
	Surface-like distorted icosahedron	4.72	5.00	1.22	4.38	

[a] Reference [19].

form $A(1-e^{-r/F})$ is chosen for $\xi(\boldsymbol{r})$, where A and F are variational parameters. We follow the approach of Fahy and co-workers to set up $\xi(\boldsymbol{r})$ [25]. Because of the statistical noise in the MC charge density, $\xi(\boldsymbol{r})$ is not generally smoothed, and this noise is removed by multiplying by a Gaussian decay factor for the Fourier components of the charge density. The random walk proceeds with 60 000 steps per particle, giving rise to a statistical error in the energy of about 0.05 eV per atom. Thus, the resulting accuracy of the relative binding energies is estimated to be within 0.05 eV per atom.

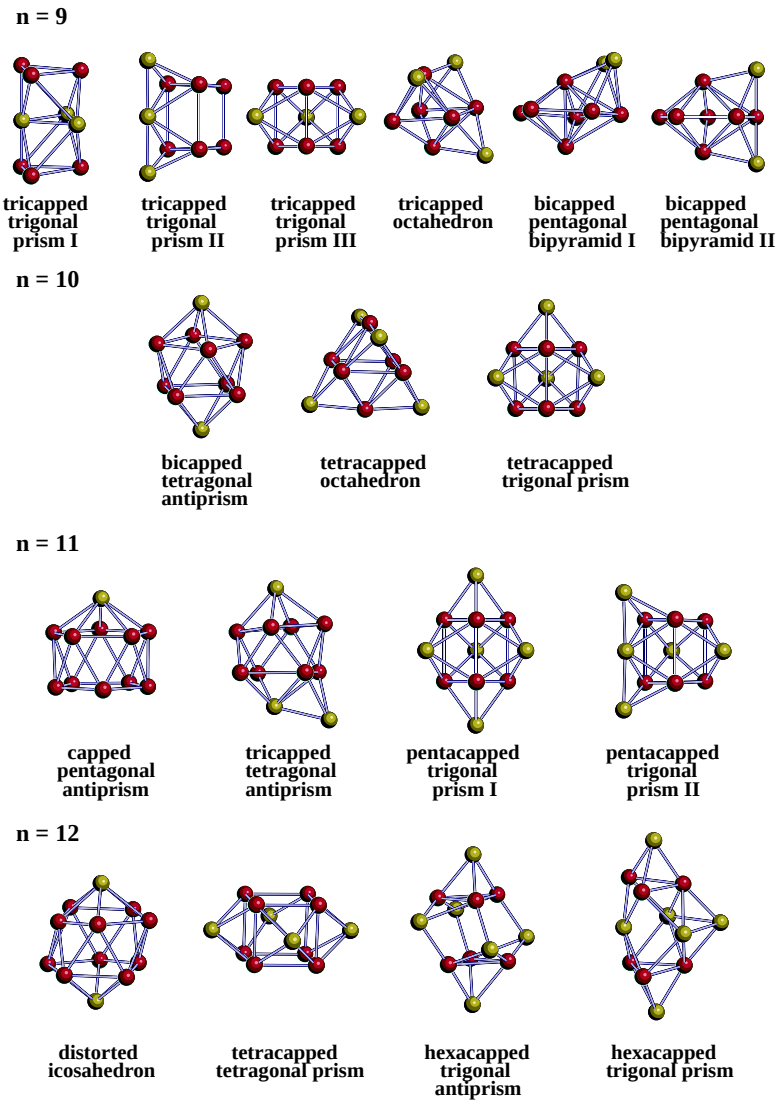

Figure 1. Various isomer structures of Si_n clusters, $9 \leqslant n \leqslant 14$.

We first examine the ground-state geometries of Si_n clusters. For the various isomers considered here (see figure 1), the LDA binding energies (E_b^{LDA}) are compared in table 1. The average bond lengths (a_0), the average coordination number ($\bar{N}_c$), and the energy gap (ΔE) between the highest occupied molecular orbital (HOMO) and the lowest unoccupied molecular orbital (LUMO) are also listed for each isomer. We choose the cut-off distance of 2.85 Å to evaluate $\bar{N}_c$.

For Si_9, we test several cluster geometries including the trigonal prism, tricapped octahedron, and bicapped pentagonal bipyramid structures. Among three different trigonal prisms, the most stable structure is found to be a tricapped prism with capping atoms on the sides, with the energy higher by 0.05 eV/atom than for a tricapped octahedron (TO). We find that the tricapped trigonal prism I undergoes large distortions, which result in

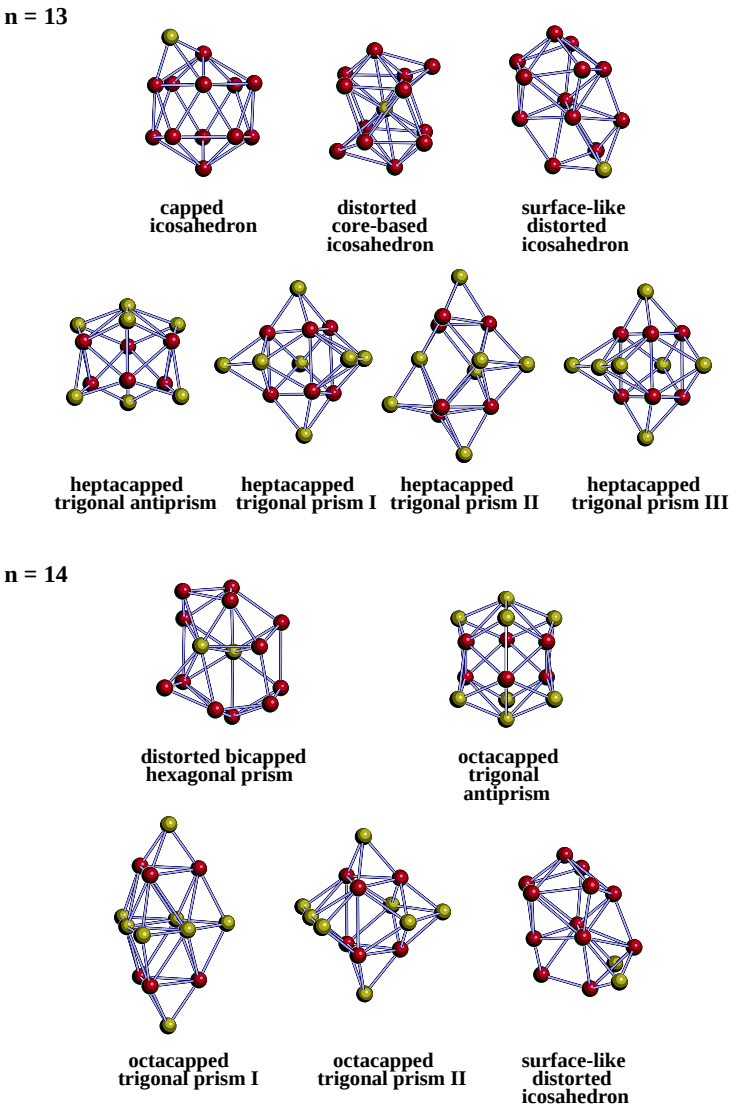

Figure 1. (Continued)

a bicapped pentagonal bipyramid I (BPB-I), as shown in figure 1. The BPB-I structure which was suggested to be the ground-state geometry [19, 26] is found to be more stable by 0.05 eV/atom than the TO structure, consistently with previous theoretical predictions [17, 19, 26]. In our calculations, we find that the equilibrium structure of Si_9 maintains a pentagonal growth pattern with bicapped atoms on the sides of the 1–5–1 pentagon (BPB-II in figure 1). The BPB-II structure is more stable by 0.07 eV/atom than the BPB-I structure, and was also found to be the lowest-energy isomer in other LDA calculations [27]. Although the average bond length and coordination number of the BPB-II structure are similar to those of other isomers, the energy gap of 2.02 eV between the HOMO and LUMO states is much higher, indicating a more covalent nature of the bonding.

Despite the many theoretical studies for Si_{10}, the equilibrium structure is not well

resolved yet. Our LDA calculations show that the most stable structure is a distorted tetracapped trigonal prism, which is more stable by 0.05 eV/atom than a tetracapped octahedron; this is similar to the result from previous molecular dynamics calculations based on the LDA [28]. In *ab initio* quantum molecular-orbital calculations [7], Raghavachari and Rohlfing suggested that the comparative stability of the tetracapped trigonal prism and the tetracapped octahedron is sensitive to the treatment of the electron correlation. However, it was shown that a more accurate treatment of the correlation does not alter the energy ordering of the two structures [19]. A bicapped tetragonal antiprism was suggested to be the equilibrium structure by classical force-field [29] and tight-binding calculations [13]. Since this structure has high D_{4d} symmetry, the energy gap is essentially zero, while a Jahn–Teller distortion reducing the symmetry to C_2 was shown to increase the energy gap by about 1 eV [17]. In our calculations, the distorted bicapped tetragonal antiprism is found to be higher in energy by 0.14 eV/atom than the stable trigonal prism, with the energy gap of 1.13 eV.

For Si_{11}, we find the stable structure to be a pentacapped trigonal prism, consistently with previous calculations [30]. The HOMO–LUMO energy gap of the pentacapped trigonal prism is estimated to be 1.80 eV, smaller than those of Si_9 and Si_{10}. Although tight-binding calculations showed that a capping of an atom on the bicapped tetragonal antiprism of Si_{10} produces the stable form of Si_{11} [17], this structure is found to be less stable by 0.03 eV/atom than the pentacapped trigonal prism. We also test an icosahedron-based structure which is derived by removing one Si atom from the ideal icosahedron consisting of 12 atoms, and find this structure to be deformed into a capped pentagonal antiprism, less stable by 0.21 eV/atom than the equilibrium geometry.

For Si_{12}, the icosahedron structure is found to be slightly distorted and more planar than its ideal geometry, and this distortion is accompanied with an increase of the energy gap by 0.72 eV. However, the distorted icosahedron is energetically less stable by 0.20 eV/atom than a hexacapped trigonal prism, which was also found to be the lowest-energy structure [11, 17]. Although the binding energy of a hexacapped trigonal antiprism is close to that of the trigonal prism, the average coordination number is much smaller, and the energy gap is reduced to 0.92 eV.

The geometry of Si_{13} is of special interest because experimentally Si_{13}^+ was observed to have lower reactivities with simple molecules than Si_n clusters with nearby values of n [8, 9, 31–33]. On the basis of an empirical interatomic potential, it was suggested that the lower chemical reactivity of Si_{13}^+ is due to the special structure of an icosahedron [10], while a trigonal antiprism was found to be more stable by *ab initio* pseudopotential calculations [18]. The core-based icosahedron with a 1–5–1–5–1 sequence of the pentagonal growth has the highest coordination number of 6.46, and is compact, exhibiting metallic bonding character. We find the core-based icosahedron to be unstable and strongly distorted, with a decrease of energy by 0.13 eV/atom, as compared to the ideal geometry. A singly capped icosahedron is also tested, and its energy is lower by 0.03 eV/atom than that of the distorted core-based icosahedron; this is similar to the tight-binding result [17]. However, the singly capped icosahedron is found to undergo large atomic relaxations, leading to a surface-like compact structure, as shown in figure 1. Although this compact structure has a small energy gap of 1.07 eV and a high average coordination number of 5.08, which are similar to the values for the icosahedral structures, its energy is lower by 0.01 eV/atom than that for a trigonal antiprism, which was considered to be the lowest-energy structure in previous calculations [18, 19]. Since the distorted core-based icosahedron is treated in our calculations, the LDA energy difference of 0.18 eV/atom between the trigonal antiprism and the distorted core-based icosahedron is smaller than the previously calculated value of 0.30 eV/atom for the high-symmetry icosahedral (I_h) geometry [19]. In our calculations, we find a new

trigonal prism as the equilibrium geometry, which is energetically more favourable by about 0.05 eV/atom than the trigonal antiprism. The energy difference between the trigonal prism and surface-like compact structures is extremely small, 0.04 eV/atom; thus, the existence of the surface-like metallic structure is highly probable, which may explain the low chemical reactivity of Si_{13}^+. It was suggested that the icosahedron can be made more stable than the prismatic structure with an adequate treatment of the electron–electron correlation beyond the LDA [20]. To see the effect of correlation energy on the energy ordering of isomers, we perform VQMC calculations for the icosahedral and prismatic structures and obtain binding energies in fairly good agreement with recent diffusion quantum Monte Carlo (DQMC) calculations [19]. Although the correlation energy was indeed found to be greater for the higher-symmetry structure [19], it is not big enough to reverse the ordering. We find that the energy ordering is nearly the same as the LDA result, as illustrated in table 1; the trigonal prism is the lowest-energy structure and the energies of the surface-like compact icosahedron and the trigonal antiprism are very close to each other. The fluctuation of the correlation energy between the LDA and VQMC calculations is estimated to be 1.0–1.2 eV, while the DQMC calculations showed a lower fluctuation of about 0.86 eV [19]. In fact, it was stated that the VQMC calculation gives 85–90% of the DQMC correlation energy for all of the clusters studied [19]. Thus, the difference of 0.14–0.34 eV between the fluctuations obtained from the two calculations results from the use of different Monte Carlo methods. The inclusion of gradient corrections to the LDA energies [34] is also tested, and the difference between the binding energies of the surface-like compact structure and the stable trigonal prism is found to remain unchanged.

For Si_{14}, we find that the equilibrium structure is a distorted capped icosahedron which is similar to the surface-like compact structure of Si_{13}. The icosahedral structure with capping atoms is strongly distorted; thus, it has a surface-like bonding character with the bond angles closely related to a metallic phase, as shown in figure 1. A similar surface-like isomer which is strongly distorted by two capping atoms on the hexagonal antiprism was also found by tight-binding molecular dynamics simulations [17]. However, trigonal prismatic structures [35] are found to be unstable compared with the surface-like compact geometry, while these structures are generally stabilized in small Si_n clusters.

It is noted that the equilibrium geometries of Si_{13} and Si_{14} have smaller energy gaps of 1.22–1.47 eV, as compared to smaller clusters ($9 \leqslant n \leqslant 12$) with the gaps ranging from 1.80 to 2.17 eV. In fact, we find that as the number of capping atoms on the trigonal prism of Si_6 increases, the energy gap decreases abruptly for $n = 13$ and 14. With five capped atoms on the trigonal and tetragonal faces of a prism, additional cappings of three atoms on the sides lead to a capped prismatic structure of Si_{14}. In this capping process, a fully capped prismatic geometry can be stabilized for Si_{11}, and a capped prismatic structure is also the stable isomer for $n = 13$, as discussed before. For Si_{14}, however, a fully capped trigonal prism is less stable than the surface-like compact geometry, although the energy difference of 0.07 eV/atom between these two structures is small. For trigonal prisms with 4–6 capping atoms, i.e., $n = 10$–12, the energy gaps are found to lie between 1.8 and 2.17 eV, while these values for the capped trigonal prisms of Si_{13} and Si_{14} decrease to 1.47 and 0.65 eV, respectively. This feature is closely related to the metallic bonding of compact structures for $n = 13$ and 14.

Next we examine a possible change of the energy ordering for different structures of ionized clusters (Si_n^+), because Si_{13}^+ and Si_{14}^+ are particularly unreactive with C_2H_4 and D_2O, while Si_{13}^+ is the cluster that is the least reactive with C_2H_4, D_2O, and O_2 [8, 9, 31–33]. For $n \leqslant 13$, the equilibrium geometries are found to remain unchanged, while for $n = 14$ a capped trigonal prismatic structure is comparable in energy to a surface-like distorted

Table 2. Calculated values for a_0 (in au), $\bar{N}_c$, ΔE (in eV), and E_b^{LDA} (in eV/atom) for Si_n^+, $9 \leqslant n \leqslant 14$.

	Structure	a_0	$\bar{N}_c$	ΔE	E_b^{LDA}
Si_9^+	Tricapped trigonal prism I	4.80	5.11	1.37	3.62
	Tricapped trigonal prism II	4.69	4.22	0.19	3.57
	Tricapped trigonal prism III	4.76	4.67	0.05	3.50
	Tricapped octahedron	4.73	4.67	0.80	3.59
	Bicapped pentagonal bipyramid I	4.79	5.11	1.31	3.62
	Bicapped pentagonal bipyramid II	4.74	4.67	1.86	3.65
Si_{10}^+	Bicapped tetragonal antiprism	4.80	4.60	1.30	3.73
	Tetracapped octahedron	4.71	4.80	1.99	3.80
	Tetracapped trigonal prism	4.72	4.60	1.64	3.82
Si_{11}^+	Capped pentagonal antiprism	4.71	4.55	0.34	3.72
	Tricapped tetragonal antiprism	4.67	4.36	0.75	3.89
	Pentacapped trigonal prism I	4.73	4.91	0.02	3.91
	Pentacapped trigonal prism II	4.70	4.91	1.74	3.90
Si_{12}^+	Distorted icosahedron	4.83	5.00	0.53	3.76
	Tetracapped tetragonal prism	4.74	4.67	0.55	3.82
	Hexacapped trigonal antiprism	4.68	4.00	0.62	3.92
	Hexacapped trigonal prism	4.73	4.67	1.91	3.93
Si_{13}^+	Distorted core-based icosahedron	4.74	4.62	0.03	3.89
	Surface-like distorted icosahedron	4.78	5.08	0.98	4.00
	Heptacapped trigonal antiprism	4.71	4.77	1.24	4.00
	Heptacapped trigonal prism I	4.71	4.77	0.81	4.00
	Heptacapped trigonal prism II	4.71	4.62	1.40	3.99
	Heptacapped trigonal prism III	4.72	4.77	1.32	4.05
Si_{14}^+	Distorted bicapped hexagonal prism	4.65	4.29	0.93	4.04
	Octacapped trigonal antiprism	4.72	4.86	0.39	4.02
	Octacapped trigonal prism I	4.88	5.57	0.46	3.93
	Octacapped trigonal prism II	4.77	5.14	0.71	4.07
	Surface-like distorted icosahedron	4.76	5.00	0.94	4.06

icosahedron (see table 2), which was shown to be the lowest-energy structural form of Si_{14}. The surface-like compact structures of Si_{13}^+ and Si_{14}^+ are found to be more stable than core-based icosahedra; this is similar to the case for neutral ion clusters. These compact structures keep the same average coordination numbers of $\bar{N}_c \approx 5.0$, but their energy gaps are slightly reduced, indicating more metallic characteristics. As shown in table 2, the energy differences between the surface-like compact and trigonal prismatic structures are very small for Si_{13}^+ and Si_{14}^+, so these clusters are also expected to be much less reactive with simple molecules than Si_n clusters with nearby values of n are. For other values, $n = 9$–12, we find that the global minima for Si_n^+ clusters are the same as those for neutral clusters, except for Si_{11}^+, for which the pentacapped trigonal prism I has the lowest energy.

Finally, we examine the electronegativity (χ) or chemical potential for Si_n^+ clusters. To remove the size dependence [36, 37], the values for $n^{1/3}\chi$, in which n is the number of atoms, are calculated and plotted as a function of n in figure 2. For $n = 11$, 13, and 14, the χ-values are found to be lower; in particular, Si_{14}^+ has the lowest electronegativity. Here the low electronegativity of Si_{11}^+ is attributed to the fact that the average coordination number of the ground-state isomer is fairly high, as shown in table 1. Since the electronegativity

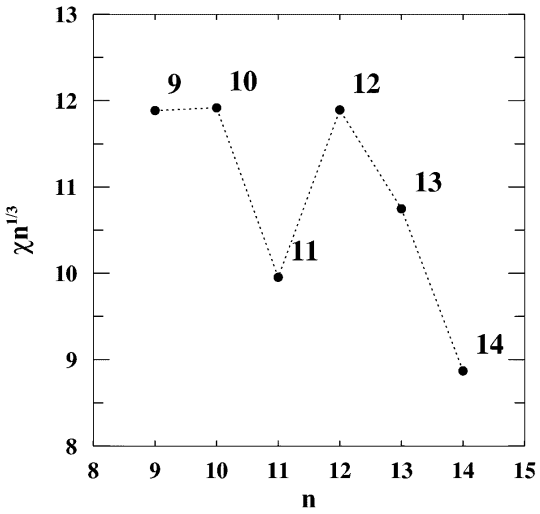

Figure 2. Electronegativities for the ground-state isomers of Si_n^+ clusters, $9 \leqslant n \leqslant 14$.

measures the tendency of electrons to escape from the system, it will be easier to remove electrons from Si_{11}^+, Si_{13}^+, and Si_{14}^+, than other Si_n^+ clusters. Thus, the low electronegativities of Si_{13}^+ and Si_{14}^+ may be the reason for these clusters having lower reactivities with simple molecules.

In conclusion, we have investigated the ground-state isomers of Si_n using the first-principles pseudopotential method, and found new equilibrium structures for $n = 12$–14. For n below 13, the trigonal prismatic structures with capping atoms are generally lower in energy than the octahedral and icosahedral structures. As n increases to 13 and 14, strongly distorted capped icosahedra with surface-like metallic bonding are found to be more stable than the core-based icosahedra, and their energies are either comparable to or lower than those of the trigonal prismatic structures. The calculated electronegativities for Si_n^+ clusters are found to be lower for $n = 11$, 13, and 14, suggesting that the surface-like structural characteristics and low electronegativities are related to the low chemical reactivities observed for Si_{13}^+ and Si_{14}^+.

Acknowledgments

This work was supported by the Ministry of Science and Technology and the CMS at Korea Advanced Institute of Science and Technology.

References

[1] Knight W D, Clemenger K, de Heer W A, Saunders W A, Chou M Y and Cohen M L 1984 *Phys. Rev. Lett.* **2** 2141
de Heer W A, Knight W D, Chou M Y and Cohen M L 1987 *Electronic Shell Structure and Metal Clusters 1987 (Solid State Physics 40)* ed H Ehrenreich and D Turnbull (Orlando, FL: Academic) p 93
[2] Röthlisberger U and Andreoni W 1991 *J. Chem. Phys.* **94** 8129
[3] Tomańek D and Schlüter M A 1986 *Phys. Rev. Lett.* **56** 1055
[4] Cheshnovsky O, Yang S H, Pettiette C L, Craycraft M J, Liu Y and Smalley R E 1987 *Chem. Phys. Lett.* **138** 119

[5] Bloomfield L A, Freeman R R and Brown W L 1985 *Phys. Rev. Lett.* **54** 2246
[6] Raghavachari K and Logovinsky V 1985 *Phys. Rev. Lett.* **55** 2853
[7] Raghavachari K and Rohlfing C M 1988 *J. Chem. Phys.* **89** 2219
[8] Creegan K M and Jarrold M F 1990 *J. Am. Chem. Soc.* **112** 3768
[9] Jarrold M F 1991 *Science* **252** 1085
[10] Chelikowsky J R and Phillips J C 1989 *Phys. Rev. Lett.* **63** 1653
[11] Bahel A and Ramakrishna M V 1995 *Phys. Rev.* B **51** 13 849
[12] Jelski D A, Swift B L, Rantala T T, Xia X and George T F 1991 *J. Chem. Phys.* **95** 8552
[13] Tomańek D and Schlüter M A 1987 *Phys. Rev.* B **36** 1208
[14] Ramakrishna M V and Pan J 1994 *J. Chem. Phys.* **101** 8108
[15] Gong X G, Zheng Q Q and He Y Z 1995 *J. Phys.: Condens. Matter* **7** 577
[16] Rantala T T, Jelski D A and George T F 1995 *Chem. Phys. Lett.* **232** 215
[17] Lee I H, Chang K J and Lee Y H 1994 *J. Phys.: Condens. Matter* **6** 741
[18] Röthlisberger U, Andreoni W and Giannozzi P 1992 *J. Chem. Phys.* **96** 1248
[19] Grossman J C and Mitáš L 1995 *Phys. Rev. Lett.* **74** 1323
[20] Phillips J C 1993 *Phys. Rev.* B **47** 14 132
[21] Ihm J, Zunger A and Cohen M L 1979 *J. Phys. C: Solid State Phys.* **12** 4409
[22] Kohn W and Sham L J 1965 *Phys. Rev.* **140** A1133
[23] Ceperley D M and Alder B J 1980 *Phys. Rev. Lett.* **45** 566
Perdew J and Zunger A 1981 *Phys. Rev.* B **23** 5048
[24] Troullier N and Martins J L 1991 *Phys. Rev.* B **43** 1993
Kleinman L and Bylander D M 1982 *Phys. Rev. Lett.* **48** 1425
[25] Fahy S, Wang X W and Louie S G 1990 *Phys. Rev.* B **42** 3503
[26] Ordejón P, Lebedenko D and Menon M 1994 *Phys. Rev.* B **50** 5645
[27] Andreoni W 1991 *Z. Phys.* D **19** 31
[28] Ballone P, Andreoni W, Car R and Parrinello M 1988 *Phys. Rev. Lett.* **60** 271
[29] Chelikowsky J R, Phillips J C, Kamal M and Strauss M 1989 *Phys. Rev. Lett.* **62** 292
[30] Rohlfing C M and Raghavachari K 1990 *Chem. Phys. Lett.* **167** 559
[31] Jarrold M F, Ray U and Creegan K M 1990 *J. Chem. Phys.* **93** 224
[32] Ray U and Jarrold M F 1991 *J. Chem. Phys.* **94** 2631
[33] Jarrold M F, Bower J E and Creegan K 1989 *J. Chem. Phys.* **90** 3615
[34] Perdew J, Chevary J A, Vosko S H, Jackson K A, Pederson M R, Singh D J and Fiolhais C 1992 *Phys. Rev.* B **46** 6671
[35] Grossman J C and Mitáš L 1995 *Phys. Rev.* B **52** 16 735
[36] March N H and Parr R G 1980 *Proc. Natl Acad. Sci. USA* **77** 6285
[37] Parr R G and Yang W 1989 *Density-functional Theory of Atoms and Molecules* (New York: Oxford University Press) p 95